Proc. Natl. Acad. Sci. USA
Vol. 93, pp. 171–175, January 1996
Genetics

Structural variation of the pseudoautosomal region between and within inbred mouse strains

DAVID KIPLING*†, HELEN E. WILSON*, ERIC J. THOMSON*, MURIEL LEE*, JOHANNA PERRY‡, STEPHEN PALMER‡, ALAN ASHWORTH‡, AND HOWARD J. COOKE*

*Medical Research Council Human Genetics Unit, Western General Hospital, Crewe Road, Edinburgh, EH4 2XU, United Kingdom; and ‡Cancer Research Campaign Centre for Cell and Molecular Biology, Chester Beatty Laboratories, Institute of Cancer Research, Fulham Road, London, SW3 6JB, United Kingdom

Communicated by M. F. Lyon, Medical Research Council, Oxon, U.K., August 14, 1995 (received for review July 3, 1995)

ABSTRACT **The pseudoautosomal region (PAR) is a segment of shared homology between the sex chromosomes. Here we report additional probes for this region of the mouse genome. Genetic and fluorescence *in situ* hybridization analyses indicate that one probe, PAR-4, hybridizes to the pseudoautosomal telomere and a minor locus at the telomere of chromosome 9 and that a PCR assay based on the PAR-4 sequence amplifies only the pseudoautosomal locus (*DXYHgu1*). The region detected by PAR-4 is structurally unstable; it shows polymorphism both between mouse strains and between animals of the same inbred strain, which implies an unusually high mutation rate. Variation occurs in the region adjacent to a $(TTAGGG)_n$ array. Two pseudoautosomal probes can also hybridize to the distal telomeres of chromosomes 9 and 13, and all three telomeres contain *DXYMov15*. The similarity between these telomeres may reflect ancestral telomere–telomere exchange.**

Pairing and exchange of DNA between the human X and Y chromosomes, which are largely different in sequence, is restricted to two small telomeric regions of homology termed pseudoautosomal regions (PARs) (1). Genetic analyses indicate that an obligatory crossover occurs in male meiosis within the main PAR (2). Failure to form the X–Y chiasma can disrupt progress of the entire chromosome set through the subsequent stages of segregation; mice with unpaired sex chromosomes show developmental arrest at metaphase I and subsequent spermatocyte degeneration (2, 3). The main human PAR extends 2.6 Mb from the short-arm telomere (1). The obligatory crossover within this PAR causes genetic markers located at the Xp/Yp telomere to show 50% recombination with sex in male meiosis (1). Occasional exchange occurs at a second human PAR found at the Xq/Yq telomere (4, 5).

The mouse PAR, located at the distal telomere, is poorly understood at the molecular level. Although its cytological behavior and role in hybrid sterility have been extensively analyzed (2), only two DNA probes for this region have been reported. The first is the $(TTAGGG)_n$ telomere repeat, which detects restriction fragment length polymorphisms that map to the PAR (6, 7). The second probe was isolated from the Mov15 transgenic mouse, which has a single Moloney murine leukemia virus integrated in the PAR (8). Proviral DNA is transferred from the X to Y chromosomes in 10–20% of male meioses, suggesting an integration site close to the PAR boundary. A sequence flanking the virus integration site, *DXYMov15*, has been cloned (9) and is a tandem repeat array of 31-bp monomer units. It is detected by the probe pMov15/1, which hybridizes to the distal telomeres of chromosomes X, Y, 4, 9, and 13 (9–12). The sex-reversed (*Sxr*) mutation (13), which involves a translocation of the male-determining region of the Y short arm to the PAR, provides another PAR marker. It shows ≈50% recombination with sex in male meiosis and is closely linked to *Sts* (14, 15).

Few genes have been localized to the mouse PAR. The phenotype of intermale aggression cosegregates with the PAR (16). Another locus is steroid sulfatase (*Sts*), mapped using variation in enzyme levels between strains (17). It has been suggested that the human and mouse PARs arose independently and are not homologous (1). Homologues of two human PAR genes, the granulocyte/macrophage colony-stimulating factor receptor α subunit gene (18) and the interleukin 3 receptor α subunit gene (19), are autosomally located in the mouse. The mouse PAR is involved in interspecific hybrid sterility. (*Mus musculus* × *Mus spretus*)F_1 females are fertile, but F_1 males are sterile and show a failure of X–Y pairing (20, 21). Genetic analysis indicates that heterozygosity for the PAR is sufficient to cause male infertility (20, 21).

Here we report additional DNA probes for the *M. musculus* PAR. One plasmid subclone, pDR484, detects the PAR telomere and two autosomes by *in situ* hybridization. Primers based on its sequence amplify only a PAR locus, *DXYHgu1*.§ However, the PCR product (PAR-4) hybridizes to another locus in addition to *DXYHgu1*; this second locus, *D9Hgu1*, is located at the distal telomere of chromosome 9 and is not amplified by these primers. The *DXYHgu1* region is structurally unstable, showing polymorphism between animals of the same inbred strain.

MATERIALS AND METHODS

Isolation of Yeast Artificial Chromosome (YAC) Subclone pDR484. pDR484 contains the 4.5-kb region of Mtel-14 (22) between the *Bam*HI cloning site and the first *Pst* I site in the insert, subcloned into pBluescript II SK⁻. *Sau*3A subclones of the insert were sequenced and compared to the European Molecular Biology Laboratory DNA data base using BLASTN (23) and conceptually translated in all six possible reading frames and compared to the National Biomedical Research Foundation protein data base using BLASTX (24). Except for short and long interspersed repetitive DNA elements, the only match was to an unpublished 86-bp mouse sequence (GenBank accession no. U14171) of unknown function. One thousand six hundred forty-one nucleotides of nonrepetitive sequence were obtained.

Pulsed-Field Gel Electrophoresis and Hybridization. PAR-4 was isolated by using the *DXYHgu1* PCR assay on pDR484. PAR-4 and pDR473 were labeled by random-priming and hybridized (25) with a final wash of 0.5× SSC at 65°C for 30 min for PAR-4 and 0.1× SSC at 65°C for 30 min

The publication costs of this article were defrayed in part by page charge payment. This article must therefore be hereby marked "*advertisement*" in accordance with 18 U.S.C. §1734 solely to indicate this fact.

Abbreviations: PAR, pseudoautosomal region; SDP, strain distribution pattern; RI, recombinant inbred; YAC, yeast artificial chromosome; cM, centimorgan.

†To whom reprint requests should be addressed.

§The sequence reported in this paper has been deposited in the GenBank data base (accession no. Z49876).

for pDR473. Fig. 3 is film autoradiography; others are Molecular Dynamics PhosphorImager images. *TelXqYq1* was scored based on the 5.7-kb C57BL/6-derived band (6). Conditions for Figs. 2, 4, and 5 were 0.9% agarose, 48 hr, 180–100 V (logarithmic scale), 6 to 2 sec (linear scale), using 0.25× TBE buffer (25) at 13°C in a Biometra Rotaphor.

BAL-31 Digestion. Twelve 35-μl C57BL/6 plugs were digested with 15 units of BAL-31 (BRL) in 1 ml of BAL-31 buffer (25). One sample was removed prior to addition of enzyme. Remaining samples were transferred to 30°C; one was removed at $t = 0$ and then at 30-min intervals for the next 4.5 hr. Plugs were washed in 10 mM Tris, pH 7.5/1 mM EDTA before *Bam*HI digestion. Pulsed-field gel conditions (Bio-Rad CHEF-DR II) were 1.0% agarose/0.5× TBE, 16 hr, 200 V, 2–4 sec switch. The filter was probed successively with PAR-4 and pDR473, a mouse genomic clone (D.K., unpublished results).

PCR Amplification. *DXYHgu1* (accession no. Z49876) was amplified by F778 (5′-AGAAACAATGGCAAGGTTGC) and F779 (5′-GCAGAAACTTTAAAATGCGAGG) designed from the pDR484 sequence. Amplification was in 25 mM Taps·HCl, pH 9.3/50 mM KCl/2 mM $MgCl_2$/0.1% Tween 20/200 μM each dNTP/0.4 μM oligonucleotides/25 ng of genomic DNA in 50 μl. Cycling conditions were 35 cycles of 94°C for 30 sec, 60°C for 45 sec, and 72°C for 30 sec followed by 72°C for 10 min.

Fluorescence *in Situ* Hybridization. pDR484 was nick-translated in the presence of biotin-16-dUTP and hybridized to CGR-8 chromosomes (26); some slides were G-banded, photographed, and destained prior to *in situ* hybridization. The probe was detected with avidin-fluorescein isothiocyanate; the counterstain was propidium iodide (Fig. 1*A*). Images were recorded using a Bio-Rad laser-scanning confocal microscope.

PAR-4 probe for fluorescence *in situ* hybridization was prepared by F778/F779 amplification of pDR484 in the above buffer containing 0.1 mM biotin-16-dUTP, 0.2 mM dATP, 0.2 mM dGTP, 0.2 mM dCTP, 2 μM dTTP, and 1 μM oligonucleotides. Hybridized probe was detected with avidin-fluorescein isothiocyanate; the counterstain was 4′,6-diamidino-2-phenylindole. Fig. 1 *B* and *C* were obtained using a Zeiss Axioplan fluorescence microscope with Photometrics charge-coupled device camera and Digital Scientific software (Cambridge, U.K.).

RESULTS

Origin of YAC Telomere-Containing Clones. We have previously described 32 $(TTAGGG)_n$-containing mouse half-YACs (22). Most were made by cloning *Bam*HI-digested *M. musculus* male DBA/2 DNA into the vector pYAC4NEONOT, which permits the cloning of terminal restriction fragments (22). Mtel-14 was chosen for further study and has ≈30 kb of insert DNA, of which less than 1.5 kb is the $(TTAGGG)_n$ array (data not shown). Four and five-tenths kb of vector-adjacent insert was subcloned to yield plasmid pDR484. This was hybridized *in situ* to chromosomes from CGR-8, a male mouse embryonic stem cell line (Fig. 1*A*). The distal telomeres of the X and Y chromosomes are labeled strongly, with additional weak labeling of the distal telomeres of chromosomes 9 and 13. This labeling is distinct from that produced by *DXYMov15* (9), which in this cell line hybridizes to the PAR telomere and to the distal telomeres of chromosomes 4 and 9 (data not shown). The chromosome 13 locus detected by pDR484 is not significantly labeled by pMov15/1, and pDR484 does not hybridize detectably to the distal telomere of chromosome 4. This was confirmed by Southern hybridization, which did not reveal any *DXYMov15* sequences in Mtel-14 (data not shown).

Partial sequence of the mouse insert of pDR484 revealed no significant similarity to any data base entry, except for short and long interspersed repetitive DNA elements, including *DXYMov15* (9, 27). PCR primers were designed to amplify the cognate locus, *DXYHgu1*, shown below to be located within the PAR. These primers amplify a 106-bp product termed PAR-4. In C57BL/6 (Fig. 1*B*) and *M. spretus* (Fig. 1*C*) PAR-4 hybridizes to the pseudoautosomal telomere.

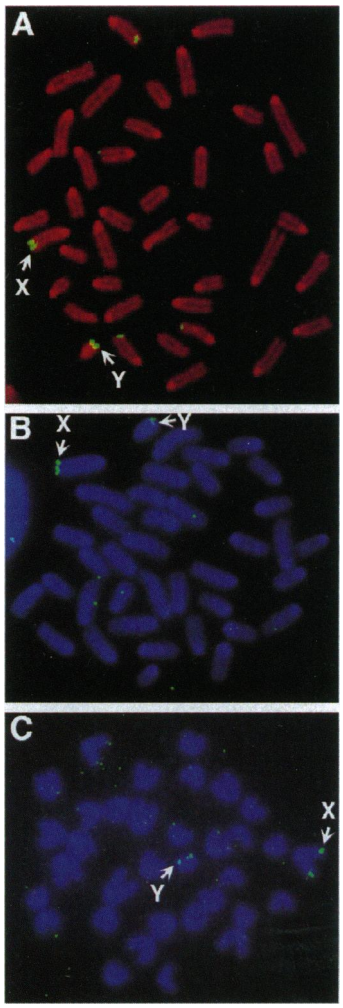

FIG. 1. *In situ* hybridization of pDR484 to the CGR-8 male mouse embryonic stem cell line (*A*) and of PAR-4 to male C57BL/6 (*B*) and *M. spretus* (*C*).

Genetic Mapping of *DXYHgu1* to the PAR. The *DXYHgu1* primers amplify a 106-bp product from *M. musculus* but not *M. spretus* genomic DNA. *DXYHgu1* was scored in the BSS panel of The Jackson Laboratory *M. musculus* × *M. spretus* interspecific backcross, mapping distal (1/94 recombinants) to *Amel*, an X-specific locus near the pseudoautosomal boundary (O. Korobova and N. Arnheim, personal communication; ref. 28). A $(TTAGGG)_n$ restriction fragment length polymorphism has been identified that maps to the PAR (6). This locus, *TelXqYq1*, maps distal (2/94 recombinants) to *Amel* in the BSB panel (7, 29). To measure the *DXYHgu1–TelXqYq1* distance in the same cross, animals of the European interspecific (EUCIB) *M. musculus* × *M. spretus* backcross (30) were typed for *DXYHgu1* and *TelXqYq1* using the panel of animals backcrossed to *M. spretus*. *DXYHgu1* shows 2/99 recombinants with *TelXqYq1*. These data indicate that *DXYHgu1* maps within the PAR, close to *TelXqYq1*.

PAR-4 Detects a Locus That Varies in Structure Within an Inbred Strain. PAR-4 is located on a terminal $(TTAGGG)_n$-containing *Bam*HI fragment in Mtel-14. Fig. 2 shows DNA from nine randomly chosen DBA/2 animals digested with *Bam*HI and probed with PAR-4. Unexpectedly, the fragment sizes are not identical. All samples show two bands of ≈25 kb and ≈60 kb. Four animals show only these two bands. How-

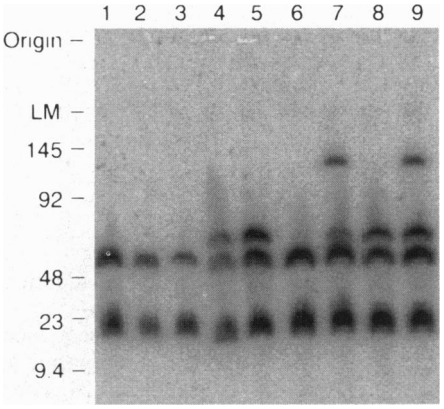

FIG. 2. *Bam*HI fragment variation between DBA/2 animals. DNA from nine randomly chosen DBA/2 animals was digested with *Bam*HI, separated by pulsed-field gel electrophoresis, and probed with PAR-4. Size markers are New England Biolabs low-range pulsed-field gel markers and *Saccharomyces cerevisiae* chromosomes. LM, limit mobility.

ever, five animals show a third band of ≈70 kb, and two of these a fourth band of ≈130 kb. Thus there can be at least a 70-kb difference in *Bam*HI fragment sizes between animals, such as between lanes 1 and 9.

Animals with three or four *Bam*HI fragments also showed additional *Pst* I and *Eco*RV fragments (data not shown). For example, the animal with two *Bam*HI bands in lane 4 of Fig. 2 releases six *Pst* I fragments. The animals in lanes 8 and 9, which show three and four *Bam*HI fragments, show two additional *Pst* I fragments of 6.6 and 25 kb. These new fragments are of equal sharpness to the other *Pst* I bands. This is inconsistent with them being terminal, because such fragments characteristically have a smeared appearance. Similarly, a sharp additional 4-kb *Eco*RV fragment was seen in animals with three and four *Bam*HI fragments (data not shown).

DBA/2 is an inbred mouse strain. Differences in the PAR-4 region among these mice suggest a significant mutation rate. In C57BL/6 × DBA/2 and C57BL/6 × C57BL/6 crosses, no new PAR-4 *Bam*HI fragments were observed in 28 F_1 offspring (data not shown). The mutation frequency therefore is relatively low, a conclusion supported by the stability of these bands for over ≈80 generations in some of the B×D recombinant inbred (RI) strains (below).

BAL-31 Exonuclease Assays. The structure of Mtel-14 suggests that PAR-4 is located over 30 kb from the end of the sex chromosomes on a potentially terminal *Bam*HI fragment. We anticipated that if any BAL-31 sensitivity was seen, it would be unlikely to remove PAR-4 signal but might shift the size of the hybridizing fragment. BAL-31 treatment followed by *Bam*HI digestion was performed on both C57BL/6 (Fig. 3) and

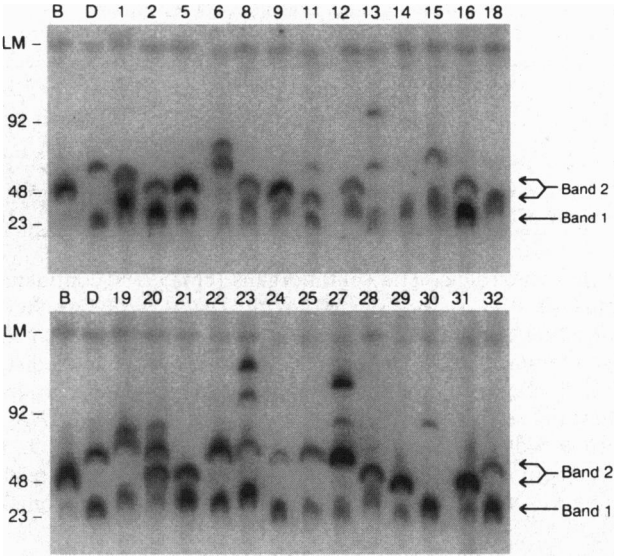

FIG. 4. *Bam*HI fragments of B×D RI strains. DNA from C57BL/6 (B), DBA/2 (D), and each B×D RI strain was digested with *Bam*HI and probed with PAR-4. Size markers are New England Biolabs low-range pulsed-field gel markers and *S. cerevisiae* chromosomes. LM, limit mobility.

DBA/2 (data not shown) genomic DNA. For both, a consistent alteration in the size of *Bam*HI fragments detected by PAR-4 is seen with increasing BAL-31 digestion. The C57BL/6 PAR-4 signal (Fig. 3 *Left*) resolves initially as a single major band. Increasing BAL-31 digestion is accompanied by the progressive appearance of signal further down, accumulating as a second band. No change in size or intensity is seen using the control probe pDR473.

Variation of PAR-4 *Bam*HI Fragments in the B×D RI Strains. The *Bam*HI fragments detected by PAR-4 are polymorphic between C57BL/6 and DBA/2 (labeled B and D in Fig. 4). These polymorphisms were mapped using the B×D RI strains (31, 32). Many B×D strains contain PAR-4 *Bam*HI fragments different from either parental allele, illustrating the structural instability of this region.

C57BL/6 (lane B) shows a strong band at ≈50 kb and a weak band at ≈25 kb. DBA/2 (lane D) shows a strong band at ≈60 kb and a second band at ≈25 kb that is stronger in intensity than the ≈25-kb C57BL/6 fragment. Each B×D strain has a fragment of ≈25 kb, with some differences in apparent size because of migration variations resulting from loading differences. This ≈25-kb band (band 1 in Fig. 4) is present as either a strong or weak band in each of the B×Ds and a strain distribution pattern (SDP) was derived based on this variation (Table 1). Ambiguous mice were not scored. This SDP shows

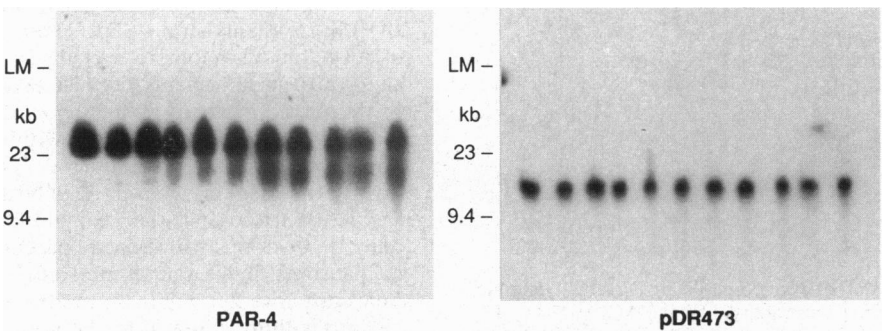

FIG. 3. BAL-31 exonuclease assay. C57BL/6 DNA was digested with BAL-31 for 0, 0, 0.5, 1, 1.5, 2, 2.5, 3, 3.5, 4, and 4.5 hr and then with *Bam*HI. The time course proceeds from left to right. The filter was separately probed with PAR-4 and pDR473. Size markers are *Hin*dIII-digested λ DNA. LM, limit mobility.

Table 1. Strain distribution patterns in B×D RI strains

	1	2	5	6	8	9	11	12	13	14	15	16	18	19	20	21	22	23	24	25	27	28	29	30	31	32
Band 1	—	D	D	**B**	B	B	B	B	B	B	B	D	B	—	B	D	D	D	D	B	B	B	B	D	B	D
Tel9q	D	D	D	**D**	B	B	B	B	B	B	B	D	—	B	B	D	D	D	D	B	B	B	B	D	B	D
Band 2	—	B	B	D	B	B	—	B	D	—	D	B	—	D	—	B	D	D	D	D	D	B	B	—	B	D
Stu I	B	B	B	D	B	B	B	B	D	—	D	—	—	—	D	B	D	D	—	D	D	B	B	—	B	D
DXNcvs4	B	B	B	D	B	B	B	B	D	D	D	B	B	D	D	B	D	D	D	D	D	—	B	B	B	D

22/23 concordance [1.2 centimorgans (cM), 95% confidence limits of 0–8.2 cM (31, 33)] with *Tel9q*, a $(TTAGGG)_n$ restriction fragment length polymorphism that maps to the distal telomere of chromosome 9 (34). *Tel9q* is the most distal marker mapped on chromosome 9 in the B×D RI strains. These data suggest that this locus, which we designate *D9Hgu1*, corresponds to the distal telomere of chromosome 9, in agreement with *in situ* data indicating that some Mtel-14 sequences are found at the distal telomere of chromosome 9 (Fig. 1*A*).

The difference in size of the upper DBA/2 and C57BL/6 bands (band 2 in Fig. 4) is a complex pattern to score because of variation in band sizes, but even so an SDP was obtained (Table 1). This shows 19/19 concordance [0 cM, 95% confidence limits of 0–6.0 cM (31, 33)] with *DXNcvs4*, which maps to the distal region of the X chromosome (35). *DXNcvs4* is the most distal X chromosome marker mapped in the B×D strains and maps proximal but close to *Amel* in The Jackson Laboratory backcross (35). The close linkage of band 2 (presumably the same locus as *DXYHgu1*) with *DXNcvs4* is consistent with it mapping to the PAR.

PAR-4 Detects a Highly Variable Locus. PAR-4 detects more than 10 *Stu* I fragments in DBA/2 (Fig. 5). Nine other inbred strains (129/SvJ, A/J, AKR/J, BALB/cJ, C3H/HeJ, C57BL/6J, DBA/1J, SJL/J, and SWR/J; data not shown) each have a different pattern, indicating a highly variable locus.

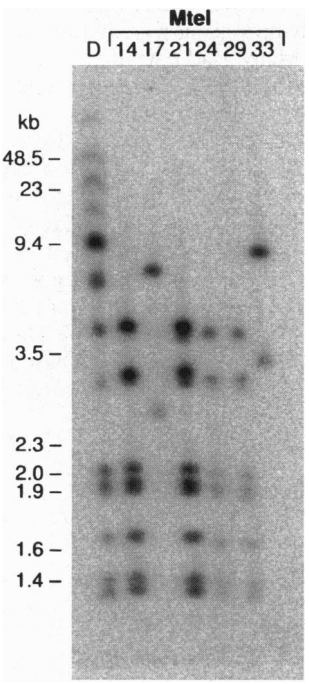

FIG. 5. Structure of Mtel YACs compared to DBA/2. Genomic DNA from DBA/2 (D) and yeast strains carrying YACs Mtel-14, -17, -21, -24, -29, and -33 were digested with *Stu* I and probed with PAR-4. Size markers are New England Biolabs low-range pulsed-field gel markers, *Hin*dIII-digested λ DNA, and *Hin*dIII plus *Eco*RI-digested λ DNA.

CBA/J and DBA/2J patterns are almost identical, possibly reflecting their ancestry (32).

Five other Mtel YACs contain PAR-4 sequences (Fig. 5). All are independent YACs derived from separate yeast transformations (22). Three YACs (Mtel-21, -24, and -29) have identical restriction maps to Mtel-14 and are *DXYHgu1* PCR positive (data not shown). We conclude that Mtel-14, -21, -24, and -29 are independent isolates of the same pseudoautosomal locus. The remaining two YACs are different in structure and are *DXYHgu1* negative and have not been studied further.

In DBA/2, PAR-4 detects seven *Stu* I fragments smaller than 4 kb (Fig. 5). Mtel-14, -21, -24, and -29 contain the same seven *Stu* I fragments (Fig. 5), indicating that these YACs faithfully represent the corresponding DBA/2 locus. The isolation of four independent $(TTAGGG)_n$-positive YACs containing these PAR-4 fragments strongly argues that these YACs are not chimeric and that these PAR-4 fragments are physically linked to $(TTAGGG)_n$ in the mouse genome.

The presence of all seven *Stu* I fragments in 30 kb of YAC insert would predict that these bands should generally cosegregate as a single locus. The *Stu* I PAR-4 pattern of the B×D RI strains was determined (data not shown). The bands did indeed cosegregate, and as with *Bam*HI (Fig. 4) some strains showed a pattern dissimilar to either a B or D allele. An SDP was obtained (Table 1) based on these small *Stu* I fragments that shows 19/19 concordance (0 cM) with *DXNcvs4* and 17/17 (0 cM) concordance with band 2. These small *Stu* I fragments in DBA/2 and C57BL/6 thus map to the PAR. Their variability in some B×D strains again demonstrates the instability of this PAR locus.

DISCUSSION

The only published probe reasonably specific for the mouse PAR is *DXYMov15*. This maps *in situ* to the PAR telomere and the distal telomeres of chromosomes 4, 9, and 13 (9–12). Our data indicate that other sequences are also shared by these telomeres. In the CGR-8 cell line pDR484 detects the PAR, 9 and 13 loci (Fig. 1*A*). pDR484 does not contain sequences homologous to *DXYMov15*, and, in CGR-8, pMov15/1 hybridizes to the PAR telomere and the distal telomeres of chromosomes 4 and 9 (data not shown). Similarly, in C57BL/6 our data indicate that PAR-4 detects the PAR and distal chromosome 9 telomeres, which are also the two major sites of *DXYMov15* in this strain (27). These shared sequences may reflect telomere–telomere exchanges in karyotype evolution but if so are ancient events, because *DXYMov15* shows a similar chromosomal distribution in *M. spretus* (12).

The PAR-4 loci are variable within an inbred strain, as shown both by DBA/2 animals (Fig. 2) and by B×D RI strains (Fig. 4). In the latter, an average of 80 generations of inbreeding have occurred since the original DBA/2 × C57BL/6 cross. Many B×D strains still show a "parental" B or D allele (Fig. 4), but some show nonparental alleles, indicating that new alleles can arise in a relatively modest number of generations.

There is little evidence for large-scale structural polymorphism at human telomeres and no evidence for the degree of structural instability described here. No large-scale polymorphism has been described for the human PAR despite a

number of long-range maps (1). Large-scale polymorphism has been reported for the human 16p telomere (36). The human population shows three sizes of alleles of the 16pter region, which vary by up to 260 kb, but no *de novo* changes have been observed. These are polymorphisms in the human population, reflecting rare mutational events millions of years ago (36). In contrast, the variation reported here is consistent with a much higher mutation rate.

What process underlies this large-scale variation? Drift in the size of a terminal $(TTAGGG)_n$ array because of turnover of telomeric sequences is inconsistent with our data in two respects. First, variation is nonterminal. Second, four different DBA/2 fragments are seen repeatedly without variation in length between animals (Fig. 2). If gradual drift produces the observed changes of up to 70 kb in size, more variability in allele size should be seen between animals. Neither length constancy nor creation of internal restriction fragments is consistent with a simple model where telomere length drift creates new variants.

We suggest instead that variation is occurring in the structure of an internal region detected by PAR-4. The exact mutational mechanism is unclear; there are multiple copies of PAR-4 and misalignment of these or other repeats and subsequent unequal crossover could create a new organization. Another possibility is recombination between nonhomologous telomeres, such as between the PAR telomere and the distal telomere of chromosome 9. Local stretches of repetitive sequence are not rare in the mouse genome, yet variation within an inbred strain is not a general feature of repeat sequence clusters, despite the potential for unequal crossover.

We thank O. Korobova and N. Arnheim for communicating results prior to publication; S. L. Bowen, D. Broccoli, N. D. Hastie, and members of the Chromosome Biology Section for commenting on the manuscript; and the Medical Research Council (MRC) Human Genome Mapping Project Resource Centre for providing European interspecific backcross DNAs. This work was supported by the MRC Human Genome Mapping Project, the Cancer Research Campaign, an MRC Training Fellowship (S.P.), and a Beit Memorial Fellowship (D.K.).

1. Rappold, G. A. (1993) *Hum. Genet.* **92,** 315–324.
2. Hale, D. W. (1994) *Cytogenet. Cell Genet.* **65,** 278–282.
3. Ashley, T., Ried, T. & Ward, D. C. (1994) *Proc. Natl. Acad. Sci. USA* **91,** 524–528.
4. Kvaløy, K., Galvagni, F. & Brown, W. R. A. (1994) *Hum. Mol. Genet.* **3,** 771–778.
5. Freije, D., Helms, C., Watson, M. S. & Donis-Keller, H. (1992) *Science* **258,** 1784–1787.
6. Eicher, E. M., Lee, B. K., Washburn, L. L., Hale, D. W. & King, T. R. (1992) *Proc. Natl. Acad. Sci. USA* **89,** 2160–2164.
7. Eicher, E. M. & Shown, E. P. (1993) *Mamm. Genome* **4,** 226–229.
8. Harbers, K., Soriano, P., Müller, U. & Jaenisch, R. (1986) *Nature (London)* **324,** 682–685.
9. Harbers, K., Francke, U., Soriano, P., Jaenisch, R. & Müller, U. (1990) *Cytogenet. Cell Genet.* **53,** 129–133.
10. Eicher, E. M., Hale, D. W., Hunt, P. A., Lee, B. K., Tucker, P. K., King, T. R., Eppig, J. T. & Washburn, L. L. (1991) *Cytogenet. Cell Genet.* **57,** 221–230.
11. Sefton, L., Arnaud, D., Goodfellow, P. N., Simmler, M.-C. & Avner, P. (1992) *Mamm. Genome* **2,** 21–31.
12. Matsuda, Y. & Chapman, V. M. (1995) *Electrophoresis* **16,** 261–272.
13. Cattanach, B. M., Pollard, C. E. & Hawkes, S. G. (1971) *Cytogenetics* **10,** 318–337.
14. Keitges, E. A., Schorderet, D. F. & Gartler, S. M. (1987) *Genetics* **116,** 465–468.
15. Nagamine, C. M., Michot, J.-L., Roberts, C., Guénet, J.-L. & Bishop, C. E. (1987) *Nucleic Acids Res.* **15,** 9227–9238.
16. Roubertoux, P. L., Carlier, M., Degrelle, H., Haas-Dupertuis, M.-C., Phillips, J. & Moutier, R. (1994) *Genetics* **135,** 225–230.
17. Keitges, E., Rivest, M., Siniscalco, M. & Gartler, S. M. (1985) *Nature (London)* **315,** 226–227.
18. Disteche, C. M., Brannan, C. I., Larsen, A., Adler, D. A., Schorderet, D. F., Gearing, D., Copeland, N. G., Jenkins, N. A. & Park, L. S. (1992) *Nat. Genet.* **1,** 333–336.
19. Miyajima, I., Levitt, L., Hara, T., Bedell, M. A., Copeland, N. G., Jenkins, N. A. & Miyajima, A. (1995) *Blood* **85,** 1246–1253.
20. Matsuda, Y., Hirobe, T. & Chapman, V. M. (1991) *Proc. Natl. Acad. Sci. USA* **88,** 4850–4854.
21. Hale, D. W., Washburn, L. L. & Eicher, E. M. (1993) *Cytogenet. Cell Genet.* **63,** 221–234.
22. Kipling, D., Wilson, H. E., Thomson, E. J. & Cooke, H. J. (1995) *Hum. Mol. Genet.* **4,** 1007–1014.
23. Altschul, S. F., Gish, W., Miller, W., Myers, E. W. & Lipman, D. J. (1990) *J. Mol. Biol.* **215,** 403–410.
24. Gish, W. & States, D. J. (1993) *Nat. Genet.* **3,** 266–272.
25. Kipling, D. & Cooke, H. J. (1990) *Nature (London)* **347,** 400–402.
26. Fantes, J. A., Bickmore, W. A., Fletcher, J. M., Ballesta, F., Hanson, I. M. & van Heyningen, V. (1992) *Am. J. Hum. Genet.* **51,** 1286–1294.
27. Takahashi, Y., Mitani, K., Kuwabara, K., Hayashi, T., Niwa, M., Miyashita, N., Moriwaki, K. & Kominami, R. (1994) *Chromosoma* **103,** 450–458.
28. Herman, G. E., Boyd, Y., Chapman, V., Chatterjee, A. & Brown, S. D. M. (1994) *Mamm. Genome* **5,** S276–S288.
29. Rowe, L. B., Nadeau, J. H., Turner, R., Frankel, W. N., Lettes, V. A., Eppig, J. T., Ko, M. S. H., Thurston, S. J. & Birkenmeier, E. H. (1994) *Mamm. Genome* **5,** 253–274.
30. European Backcross Collaborative Group (1994) *Hum. Mol. Genet.* **3,** 621–628.
31. Taylor, B. A. (1978) in *Origins of Inbred Mice*, ed. Morse, H. C. (Academic, New York), pp. 423–438.
32. Lyon, M. F. & Searle, A. G. (1989) *Genetic Variants and Strains of the Laboratory Mouse* (Oxford Univ. Press, Oxford), 2nd Ed.
33. Silver, J. (1985) *J. Hered.* **76,** 436–440.
34. Elliott, R. W. & Yen, C.-H. (1991) *Mamm. Genome* **1,** 118–122.
35. Hayashizaki, Y., Hirotsune, S., Okazaki, Y., Shibata, H., Akasako, A., Muramatsu, M., Kawai, J., Hirasawa, T., Watanabe, S., Shiroishi, T., Moriwaki, K., Taylor, B. A., Matsuda, Y., Elliott, R. W., Manly, K. F. & Chapman, V. E. (1994) *Genetics* **138,** 1207–1238.
36. Wilkie, A. O. M., Higgs, D. R., Rack, K. A., Buckle, V. J., Spurr, N. K., Fischel-Ghodsian, N., Ceccherini, I., Brown, W. R. A. & Harris, P. C. (1991) *Cell* **64,** 595–606.